



In silico mutation of aromatic with aliphatic amino acid residues in *Clostridium perfringens* epsilon toxin (ETX) reduces its binding efficiency to Caprine Myelin and lymphocyte (MAL) protein receptors

Sunil Kumar, Santosh Kumar Behera, Kumaresan Gururaj, Anurag Chaurasia, Sneha Murmu, Ratna Prabha, U. B. Angadi, Rajveer Singh Pawaiya & Anil Rai

To cite this article: Sunil Kumar, Santosh Kumar Behera, Kumaresan Gururaj, Anurag Chaurasia, Sneha Murmu, Ratna Prabha, U. B. Angadi, Rajveer Singh Pawaiya & Anil Rai (2023): *In silico* mutation of aromatic with aliphatic amino acid residues in *Clostridium perfringens* epsilon toxin (ETX) reduces its binding efficiency to Caprine Myelin and lymphocyte (MAL) protein receptors, Journal of Biomolecular Structure and Dynamics, DOI: [10.1080/07391102.2023.2204362](https://doi.org/10.1080/07391102.2023.2204362)

To link to this article: <https://doi.org/10.1080/07391102.2023.2204362>



View supplementary material [↗](#)



Published online: 02 May 2023.



Submit your article to this journal [↗](#)



View related articles [↗](#)



View Crossmark data [↗](#)



In silico mutation of aromatic with aliphatic amino acid residues in *Clostridium perfringens* epsilon toxin (ETX) reduces its binding efficiency to Caprine Myelin and lymphocyte (MAL) protein receptors

Sunil Kumar^{a*}, Santosh Kumar Behera^{b*}, Kumaresan Gururaj^{c*}, Anurag Chaurasia^d, Sneha Murmu^a, Ratna Prabha^a, U. B. Angadi^a, Rajveer Singh Pawaiya^c and Anil Rai^a

^aICAR-Indian Agricultural Statistics Research Institute, New Delhi, India; ^bNational Institute of Pharmaceutical Education and Research, Ahmedabad, India; ^cICAR-Central Institute for Research on Goats, Makhdoom, Mathura, India; ^dICAR-Indian Institute of Vegetable Research, Varanasi, India

Communicated by Ramaswamy H. Sarma

ABSTRACT

Enterotoxaemia (ET) is a severe disease that affects domestic ruminants, including sheep and goats, and is caused by *Clostridium perfringens* type B and D strains. The disease is characterized by the production of Epsilon toxin (ETX), which has a significant impact on the farming industry due to its high lethality. The binding of ETX to the host cell receptor is crucial, but still poorly understood. Therefore, the structural features of goat Myelin and lymphocytic (MAL) protein were investigated and defined in this study. We induced the mutations in aromatic amino acid residues of ETX and substituted them with aliphatic residues at domains I and II. Subsequently, protein-protein interactions (PPI) were performed between ETX (wild)-MAL and ETX (mutated)-MAL protein predicting the domain sites of ETX structure. Further, molecular dynamics (MD) simulation studies were performed for both complexes to investigate the dynamic behavior of the proteins. The binding efficiency between 'ETX (wild)-MAL protein' and 'ETX (mutated)-MAL protein complex' interactions were compared and showed that the former had stronger interactions and binding efficiency due to the higher stability of the complex. The MD analysis showed destabilization and higher fluctuations in the PPI of the mutated heterodimeric ETX-MAL complex which is otherwise essential for its functional conformation. Such kind of interactions with mutated functional domains of ligands provided much-needed clarity in understanding the pre-pore complex formation of epsilon toxin with the MAL protein receptor of goats. The findings from this study would provide an impetus for designing a novel vaccine for Enterotoxaemia in goats.

ARTICLE HISTORY

Received 19 December 2022
Accepted 11 April 2023

KEYWORDS

Epsilon toxin (ETX); enterotoxaemia (ET); MAL protein; protein-protein interactions; molecular dynamics

Introduction

The pore-forming aerolysin-like toxin known as Epsilon toxin (ETX) is produced by *Clostridium perfringens* type B and D. It is produced in a form of a protoxin with a size of ~33kDa but processed in the system to an active form by proteolytic digestion of host trypsin, α -chymotrypsin or λ -protease produced by *C. perfringens* itself that break away 11–14 amino acid and 22–29 amino acid residues from the N-terminal end and the C-terminal end respectively (Bokori-Brown et al. 2013). The ETX is coded by the epsilon-toxin (*etx*) gene present in the extra-chromosomal plasmids of *C. perfringens* which are transferred intra-species by conjugation, facilitating the expression of virulence (Mathur et al., 2010). After botulinum and tetanus, ETX ranks as the third most potent toxin, primarily responsible for clinical manifestation of enterotoxaemia in goats. The toxin permeates through the gut mucous membrane traversing through the circulatory system reaching various organs like heart, kidney, lungs and even crossing the blood-brain barrier (BBB) and reaching to the

brain (Finnie & Uzal, 2022). The ETX has three domains viz., I, II and III made up of beta-sheets and has structural and conformational similarity with other pore-forming toxins like aerolysin (*Aeromonas hydrophila*), parasporin-2 (Ps2, produced by *Bacillus thuringiensis*), LSL (Lectins produced by *Laetiporus sulphureus*), although the sequence similarity is much less (Khalili et al., 2017). Certain aromatic amino acid residues present in the domain-I and II mediates primary interaction of the toxin with the host receptors, and therefore mutation in these domains with aliphatic residues could weaken the interaction with the host. Also the domain-I specifically has tryptophan residue which engineers the receptor-binding. While Domain-III present in the c-termini blocks the heptamerization process essential for host cell membrane insertion by the toxin while in protoxin form. On the contrary the activated ETX could bind to cell receptors and initiate the heptameric complexes formation followed by insertion into the membrane in the form of pores, which is dependent upon cholesterol. The sialidases produced by *C. perfringens* aids in its adhesion to

colonize the intestinal epithelium which in turn also promotes the sensitivity of host cells to ETX by exposing maximal receptor area both quantitatively and numerically. In nutshell the toxin enters the host cell membrane by three distinct process viz., (1) Binding to cell membrane through receptor, (2) Heptamerization and formation of pre-pore complex of 155 kDa culminating to insertion into the cell membrane and (3) Pore formation by heptamers which allows depletion of potassium ion and ATP molecules thereby disrupting the cytosolic ionic balance finally leading to cell death.

Previously, the receptors for ETX were studied in detail and hypothesized that they bind to the lipid rafts made up of cholesterol or sphingomyelin also termed as detergent-resistant domains (DRM) of the Madine Darby canine kidney (MDCK) cells. Recently, it has been discovered that the tyrosine residues of Epsilon toxin (ETX) can bind to hepatitis A virus cellular receptor 1 (HAVCR1), resulting in toxicity and consequent pathogenesis (Dorca-Arévalo et al., 2022). Consequently other receptors including myelin and lymphocyte protein (MAL) and caveolin-1 (CAV1) ETX-MAL complex interacts with TMEM16 proteins which function as ATP dependent calcium activated chloride transmembrane channels (Nagahama et al., 2020). Blanch et al. (2018) have identified a crucial tetraspanning membrane protein MAL with a molecular weight of 17 kDa responsible for the cytotoxic impact of ETX. In other words, for the ETX-MAL in order to produce the toxic effects requires an increment in the intracellular calcium concentration. Similarly, CAV1 and CAV2 were also found to be essential for ETX activity in the host cells as caveolin-deficient cells were resistant to the toxins due to reduced oligomerization (Fennessey et al., 2012).

The surface amino acid residues in the domain-I of ETX plays an important role (Bokori-Brown et al., 2013; Dorca-Arévalo et al., 2022) in its binding to the host cell receptors. Any mutations or substitutions could relatively weaken the pre-pore formation steps for which the 'binding' is a most critical step that initiates the cellular pathogenesis. Alterations in the key residues of ETX were conducted using both *in silico* (Khalili et al., 2017) and wet-lab (Dorca-Arévalo et al., 2022) and the protein-protein interactions were studied. However, the most important receptor for ETX viz., MAL and its interactions studied revealed the role of surface aromatic residues in Domain-I and II in binding to cell membrane. In this study, we have utilized the molecular modeling technique in conjunction with MD simulations to investigate how ETX and MAL proteins bind together, as well as explored that how epsilon toxin affects the physio-biochemical and molecular mechanisms in goats. Further we have reported the *in silico* structural and functional analysis of 'ETX (wild)-MAL protein' and 'ETX (mutated)-MAL protein complex' models and its effect on binding and generation of hydrogen bonds. Such kind of interactions with mutated functional domains of ligand could elucidate the molecular events underlying the interaction of epsilon toxin with the goats' MAL protein receptor. In future, such *in silico* bioinformatics analysis could aid in tapping the key molecular events underlying the host-pathogen interaction, thereby leading to identification of the key epitopes

and its functional modulations in designing an effective vaccine for Enterotoxaemia in goats.

Material and methods

Sequence, structure and functional analysis

The UniProtKB database was utilized to obtain the Epsilon toxin (ETX) sequence, structural, and functional information of *Clostridium perfringens* with ID Q02307 (ETXB_CLOPF), and the NCBI database was used to obtain the Myelin and lymphocyte protein (MAL) information from *Capra hircus* (goat) with accession number XP_017910309.1. The X-ray diffraction structure of ETX (PDB ID 1UYJ), comprised of 296 (16-295) amino acids in length with a resolution of 2.60 Å were retrieved from the PDB database.

Model generation and validation

The 3D structure of MAL was not available in the Protein Data Bank (PDB), hence it was predicted by implementing an advanced modeling protocol. To construct the 3D models of MAL, the threading method of protein modeling was utilized, with the aid of I-TASSER Server (Zhang, 2008). The validation of the predicted models was performed on the SAVES Server (Colovos & Yeates, 1993; Hooft et al., 1996; Laskowski, MacArthur, Moss, & Thornton, 1993; Pontius et al., 1996; Vaguine et al., 1999; Zhang et al., 2011). Further, the predicted models were refined using the ModRefiner (Xu & Zhang, 2011). The energy minimization of the refined model was carried out using the CHARMM force field. The steepest descent algorithm was initially used for energy minimization, followed by conjugate gradient algorithm to achieve the convergence (Weng et al., 2005).

Structure refinement

The 3D structure of ETX obtained from PDB was found to be incomplete due to the presence of several missing residues. To address this issue, the Protein Preparation wizard in Schrodinger Maestro v 2022.4 was employed to fill the gaps in the ETX structure.

Protein-protein interactions

Protein-protein interactions (PPIs) pose a significant challenge in modern biology due to their crucial role in various biochemical processes. To analyze the PPIs of Epsilon toxin proteins and MAL protein of goat, protein-protein docking was performed using the online Hawk Dock server. This server is a robust tool that can predict binding structures and identify the key residues involved in PPIs. The HawkDock server was utilized by uploading the PDB format of both proteins in four different combinations, which included non-simulated ETX (wild) with non-simulated MAL, non-simulated ETX (mutated) with non-simulated MAL, pre-simulated ETX (wild) with pre-simulated MAL, and pre-simulated ETX (mutated) with pre-simulated MAL. The advanced option of re-ranking top 10 models by MM/GBSA

was selected to determine the best docked complex based on the best binding free energy. The best docked complex was characterized and subjected to further computational analysis based on binding energy values, intermolecular hydrogen (H)-bonds, as well as other hydrophobic and electrostatic interactions. The presence of intermolecular bonds between protein-protein interaction complexes was demonstrated using DimPlot.

Prediction of domain sites

In terms of structure, folding, function, evolution, and even design, proteins can be broken down into their component domains. For protein classification, biological function comprehension, annotation of evolutionary mechanisms, and protein design knowledge of protein domains are essential. By grouping the protein sequences into families and estimating the presence of domains and crucial locations, the database InterPro (Mitchell et al., 2015) enabled the functional analysis of protein sequences. In the current investigation, InterPro-EMBL-EBI (InterPro database (<http://www.ebi.ac.uk/interpro/>)) was used to identify the key domain sites of ETX protein.

Mutation of aromatic to aliphatic amino acids

The existing reports state that certain aromatic amino acids residues present in the domain-I and II mediates primary interaction of the toxin with the host receptors, and mutation in these domains by aliphatic residues could weaken the interaction with the host. Therefore, necessary mutations were performed in ETX protein by substituting the aromatic amino acids with the aliphatic amino acids at its respective positions in wild type using BIOVIA Discovery Studio 4.5 Visualizer (BIOVIA, San Diego, CA, USA).

Molecular dynamics (MD) simulations

MD is an advanced computational tool that predicts and analyzes physical movements of atoms and molecules during macromolecular structure-to-function interactions. It allows atoms and molecules to interact for a specific time, illustrating the dynamic 'evolution' of the system (Durrant & McCammon, 2011). In order to confirm the binding modes of macromolecules and to obtain a comprehensive impression of protein-protein complexes, MD simulations of ETX (wild), ETX (mutated), MAL, ETX (wild)-MAL, ETX (mutated)-MAL, pre-simulated ETX (wild)-pre-simulated MAL, and pre-simulated ETX (mutated)-pre-simulated MAL complexes were performed using the Desmond program. The top four heterodimeric protein-protein complexes from HawkDock were subjected to 100 ns of MD simulation. The MD protocol followed a series of steps including minimization, heating, equilibration, and production run. The protein-protein complexes were minimized using the OPLS4 force field and topology and atomic coordinates were obtained automatically. The compound was then placed in an SPC solvent model orthorhombic box ($15 \times 15 \times 10 \text{ \AA}$), and the physiological pH was neutralized by adding 0.15 M NaCl. The water box was configured using the

Particle Mesh Ewald (PME) boundary condition to ensure that no solute atoms occurred within 10 \AA distance of the border. The entire system was simulated at 300 K for 100 ns using the NPT ensemble. The structural alterations and dynamic behaviour of the protein were analyzed using root mean square deviation (RMSD) and root mean square fluctuation (RMSF) graphs. RMSD measures the difference between the backbones of a protein from its initial structural conformation to its ultimate position, while RMSF identifies the flexible regions of a protein or complex (Aier et al., 2016). Intermolecular bonds between protein-protein interaction complexes were visualized using DimPlot.

Principal component analysis (PCA)

Essential Dynamics (ED) or Principal Component Analysis (PCA) is a statistical technique that reduces the high-dimensional motional data sets into a small subset of principal components (PCs), separating collective motions from local dynamics and finally defining it. Essential dynamics (ED) approach was used to perform PCA, with the `essential_dynamics.py` tool at Desmond module of Schrodinger Maestro v 2022.4 to accomplish the coordinated motions in the Apo, and Holo states of the proteins.

Results

Screening of domain sites

The InterPro-EMBL-EBI database has revealed the presence of I, II and III domains in ETX protein at various locations. The amino acids from 16 to 67 of ETX protein codes for Domain I, & II and the rest codes for domain III (Figure S2a and S2b).

Model generation and mutation of aromatic amino acids to aliphatic (Alanine)

I-TASSER generated five models, and the best one(s) was selected based on the C-score. The selected model was validated using SAVES server, considering various parameters. The final model obtained was found to be stable (Figure S1a and S1b and Table S1).

Considering the existing reports on strong interactions between toxin (ETX) and host mediated by certain aromatic amino acids residues present in the domain-I and II of toxin protein, mutations were performed at positions Tyr17, Tyr29, Tyr33, Tyr35, Tyr 42, Tyr 43, Tyr49, Phe50, Phe62, Tyr63 of ETX domain I and II with alanine residues which could weaken the interaction with the host.

Molecular rigid docking

HawkDock web server produced 10 highest-ranked models of protein-protein interaction (PPI) with varying binding energies for each of the four combinations (non-simulated ETX (wild) with non-simulated MAL, non-simulated ETX (mutated) non-simulated MAL, pre simulated ETX (wild) with pre-simulated MAL, pre-simulated ETX (mutated) with pre-simulated MAL). The non-simulated ETX

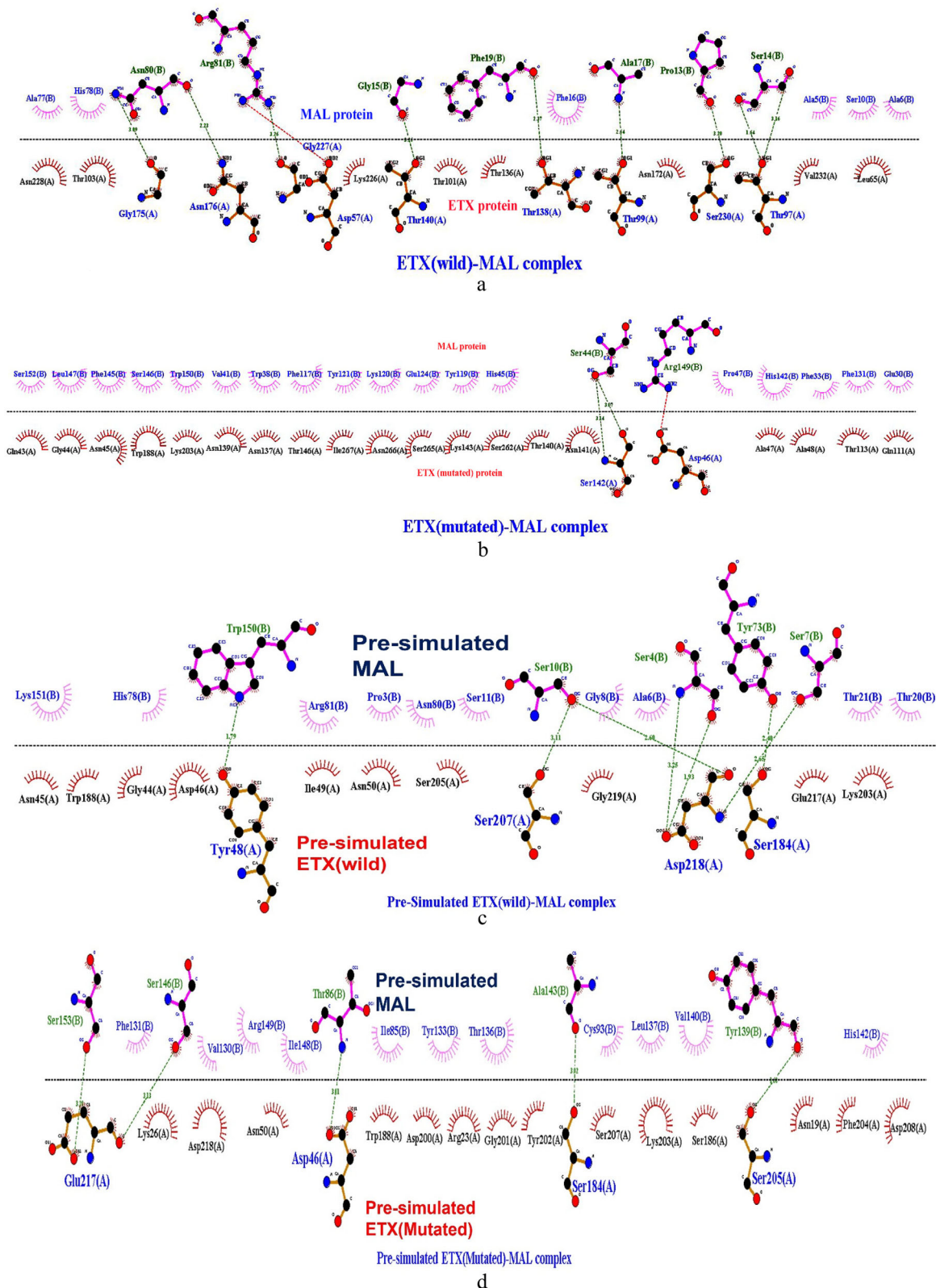


Figure 1. (a) The protein–protein interaction of non-simulated Epsilon toxin (ETX-wild) with non-simulated Myelin and lymphocyte (MAL) protein. (b) The protein–protein interaction of non-simulated Epsilon toxin (ETX-mutated) with non-simulated Myelin and lymphocyte (MAL) protein. (c) The protein–protein interaction of pre-simulated Epsilon toxin (ETX-wild) with pre-simulated Myelin and lymphocyte (MAL) protein. (d) The protein–protein interaction of pre-simulated Epsilon toxin (ETX-mutated) with pre-simulated Myelin and lymphocyte (MAL) protein.

(wild) with non-simulated MAL, non-simulated ETX (mutated) non-simulated MAL, pre simulated ETX (wild) with pre-simulated MAL, pre-simulated ETX (mutated) with pre-simulated MAL protein complex models with highest binding affinity -50.22 kcal/mol,

-52.49 kcal/mol, -31.45 kcal/mol and -33.85 kcal/mol were selected for further computational analysis. The PPI heterodimeric non-simulated ETX (wild) with non-simulated MAL protein docked complex (Figure 1a and Figure S4A) revealed nine Hydrogen

bonds with an average of $\sim 3.057 \text{ \AA}$ which signifies the strong interaction between both the proteins, the PPI heterodimeric non-simulated ETX (mutated) non-simulated MAL protein docked complex (Figure 1b; Figure S4B) revealed one salt bridge and three Hydrogen bonds with an average of $\sim 3.120 \text{ \AA}$. Compared to wild-type, mutated complex had a smaller number of H bonds, signifying a decrease in interaction with host protein. Similarly, the PPI heterodimeric pre-simulated ETX (wild) with pre-simulated MAL (Figure 1c; Figure S5A), represented seven Hydrogen bonds with an average of $\sim 2.962 \text{ \AA}$. Compared to pre simulated wild, pre-simulated ETX (mutated) with pre-simulated MAL protein complex represented four Hydrogen bonds with an average of $\sim 3.089 \text{ \AA}$ (Figure 1d; Figure S5B).

Trajectory analysis of MD simulations

In the current investigation, we have employed the MD simulations of eight systems ETX (wild), ETX (mutated), MAL, PPI heterodimeric complex of non-simulated ETX (wild) with non-simulated MAL, non-simulated ETX (mutated) non-simulated MAL, pre simulated ETX (wild) with pre-simulated MAL, pre-simulated ETX (mutated) with pre-simulated MAL using Desmond suit (Schrödinger Release 2022-4: Maestro, Schrödinger, LLC, New York, NY, 2022) in order to understand the dynamic behaviour, and mode of binding in all the systems. The targeted proteins and protein-protein complex structures were considered from the final docked structures, as discussed above. To evaluate the stability of the docked complexes and receptor structural rearrangements, a 100 ns MD simulation was conducted. The dynamic stability of both the complexes was determined by analyzing the RMSD profile of the backbone atoms at 100 ns, as depicted in Figure 2(A)–(D).

The backbone RMSD graph of heterodimeric non-simulated ETX (wild)-MAL complex revealed a stable trajectory after 40 ns of simulation upon comparison with non-simulated heterodimeric ETX (mutated)-MAL complex which exhibited even higher deviations after 40 ns. The non-simulated heterodimeric ETX (wild)-MAL complex depicted a stable trajectory with RMSD value between ~ 3.6 and $\sim 5.0 \text{ \AA}$ after 40 ns as compared to the heterodimeric non-simulated ETX (mutated)-MAL complex with RMSD value between ~ 2.6 and $\sim 6.8 \text{ \AA}$ from 40 to 100 ns. This suggests that those mutations may have destabilizes the protein-protein interactions by changing its conformation. Similarly, the heterodimeric pre-simulated ETX (wild)-MAL complex revealed a stable trajectory up to 80 ns of simulation upon comparison with non-simulated heterodimeric pre-simulated ETX (mutated)-MAL complex which exhibited higher deviations throughout the simulation time period with RMSD value between ~ 2.0 and $\sim 9.8 \text{ \AA}$. This again suggests that those mutations may have destabilizes the protein-protein interactions by changing its conformation.

To validate the RMSD result, RMSF was used to observe the mobility of residues in both states. RMSF plots were created for this purpose, as shown in Figure 3(A)–(D) and Figure S6.

Overall, the heterodimeric non-simulated ETX (mutated)-MAL complex exhibited higher fluctuations than the heterodimeric non-simulated ETX (wild)-MAL complex, indicating restricted movements in the wild state throughout the

simulation. In the mutated state, amino acid residues 20–25, 60–90, 180–210, and 285–300 showed greater deviations in their $C\alpha$ atoms compared to other regions, possibly due to weaker interactions. Similarly, the heterodimeric pre-simulated ETX (mutated)-MAL complex showed higher fluctuations than the heterodimeric pre-simulated ETX (wild)-MAL complex. Approximately 10 terminal residues from both the C- and N-terminal ends displayed greater deviations in both states, which can be ignored. The RMSF plots suggest that the mutations increase the mobility of residues in the mutated state.

The secondary structure elements (SSE) distribution by residue index of intermolecular heterodimeric pre-simulated ETX (wild)-MAL and pre-simulated ETX (mutated)-MAL complexes for each trajectory frame over the course of the simulation, and monitoring of each residue and its SSE assignment over time are represented in Figure S3(a)–(d).

H-bond analysis

The course of MD simulations was used to track the intermolecular hydrogen bonds of both the wild and mutated complex states, as shown in Figure 4(A)–(D). Throughout the simulation time, a variable number of intermolecular hydrogen bonds were observed in all four wild and mutated complexes of both non-simulated and pre-simulated states during the post-MD analysis. Nine H-bonds with an average atomic distance of $\sim 2.918 \text{ \AA}$ was represented in case of Post MDS of non-simulate ETX (wild)-MAL complex, and three H-bonds with average atomic distance of $\sim 2.958 \text{ \AA}$ in case of Post MDS of non-simulate ETX (mutated)-MAL complex was depicted. Similarly, two H-bond with an average atomic distance of $\sim 2.791 \text{ \AA}$ was represented in case of Post MDS of pre-simulate ETX(wild)-MAL complex and seven H-bonds with an average atomic distance of $\sim 3.050 \text{ \AA}$ was represented in case of Post MDS of pre-simulate ETX(mutated)-MAL complex.

The number of H-bonds was directly proportional to the stability of the complex over the entire simulation time. During simulations of heterodimeric non-simulated ETX (wild)-MAL complex, H-bonds forming residues such as Thr97, Thr140, Ser230, Thr99, Gly175, Asn176, and Val177 of ETX (wild) were broken, but later novel H-bond (Tyr64, Thr136, Tyr64, Thr97, Thr138, Asn137, Asn228, Ser230), salt bridge, van der Waals and hydrophobic contacts were compensated (Figure 4A). Thr138 did not compensate which indicates its importance in stabilizing the toxin-host interaction. Similarly, heterodimeric non-simulated ETX (mutated)-MAL complex, H-bonds forming residues such as Ser 142 of ETX (mutated) was broken, but later novel H-bond (Ser130, ILE49) van der Waals and hydrophobic contacts were compensated (Figure 4B). Gln43 did not compensate which indicates its importance in stabilizing the toxin-host interaction. In case of pre-simulated ETX (wild)-MAL complex, H-bonds forming residues such as Tyr48, Ser184, Ser207, Asp218 of ETX (wild) were broken, but later novel H-bond (Ile49, Phe47), salt bridge, van der Waals and hydrophobic contacts were compensated (Figure 4C), whereas of pre-simulated ETX (mutated)-MAL complex, H-bonds forming residues such as Asn19, Ser184, Glu217 of ETX

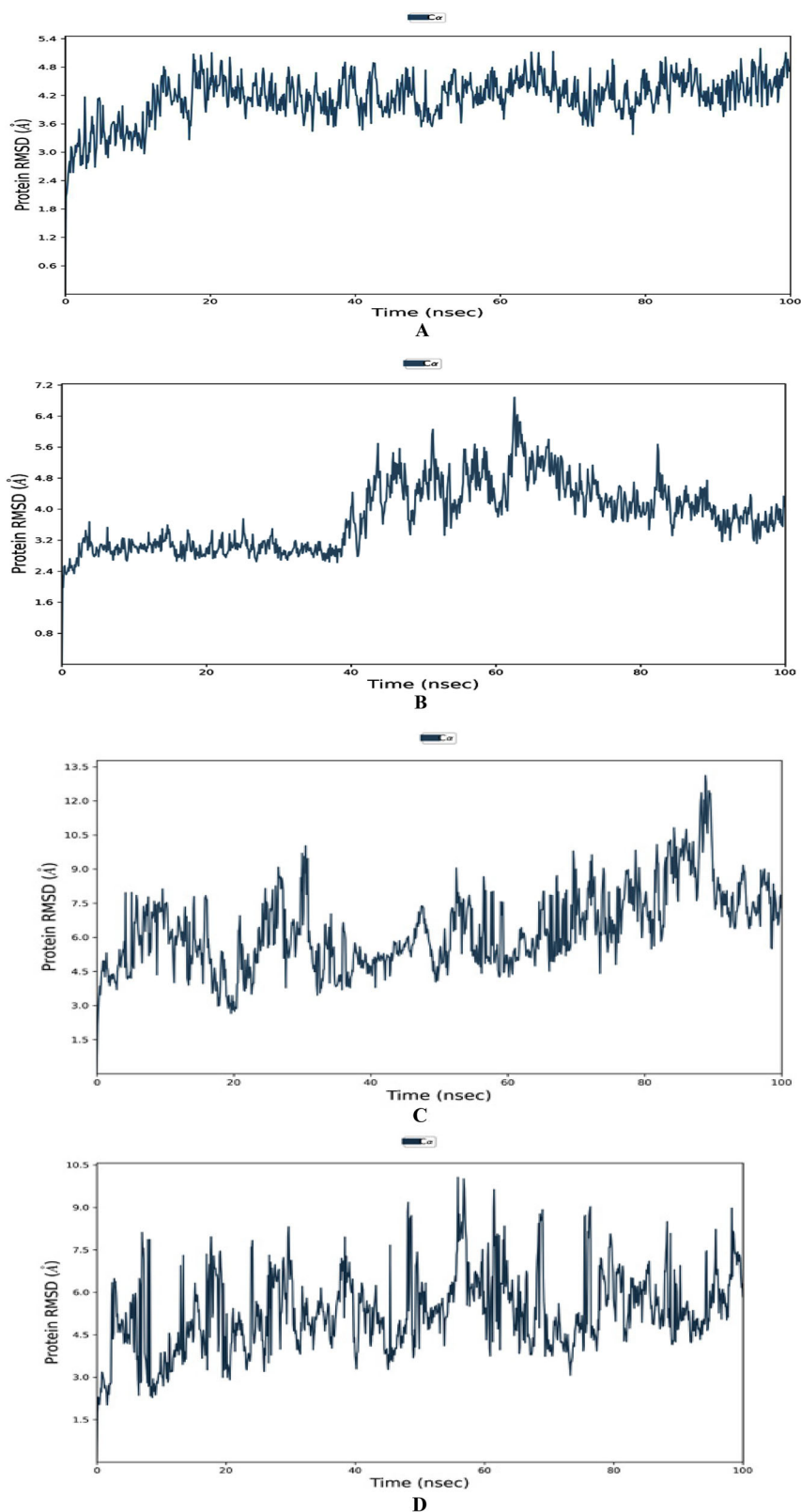


Figure 2. (A) RMSD plot of heterodimeric non-simulated ETX (wild)-MAL complex in MD simulation study. (B) RMSD plot of heterodimeric non-simulated ETX (mutated)-MAL complex in MD simulation study. (C) RMSD plot of heterodimeric pre-simulated ETX (wild)-MAL complex in MD simulation study. (D) RMSD plot of heterodimeric pre-simulated ETX (mutated)-MAL complex in MD simulation study.

(mutated) were broken, but later novel H-bond (Arg23, Ser186, Ser205, Asn51), salt bridge, van der Waals and hydrophobic contacts were compensated (Figure 4D). Asp46 did not compensate which indicates its importance in stabilizing the toxin-host interaction.

The post MD analysis depicted a change in the number of hydrogen bonding residues in all states, but there was a formation of salt bridge in post MDS of non-simulated wild state and deletion of salt bridge in post MDS of non-simulated mutated state. Subsequently, a salt bridge was found in both post MDS

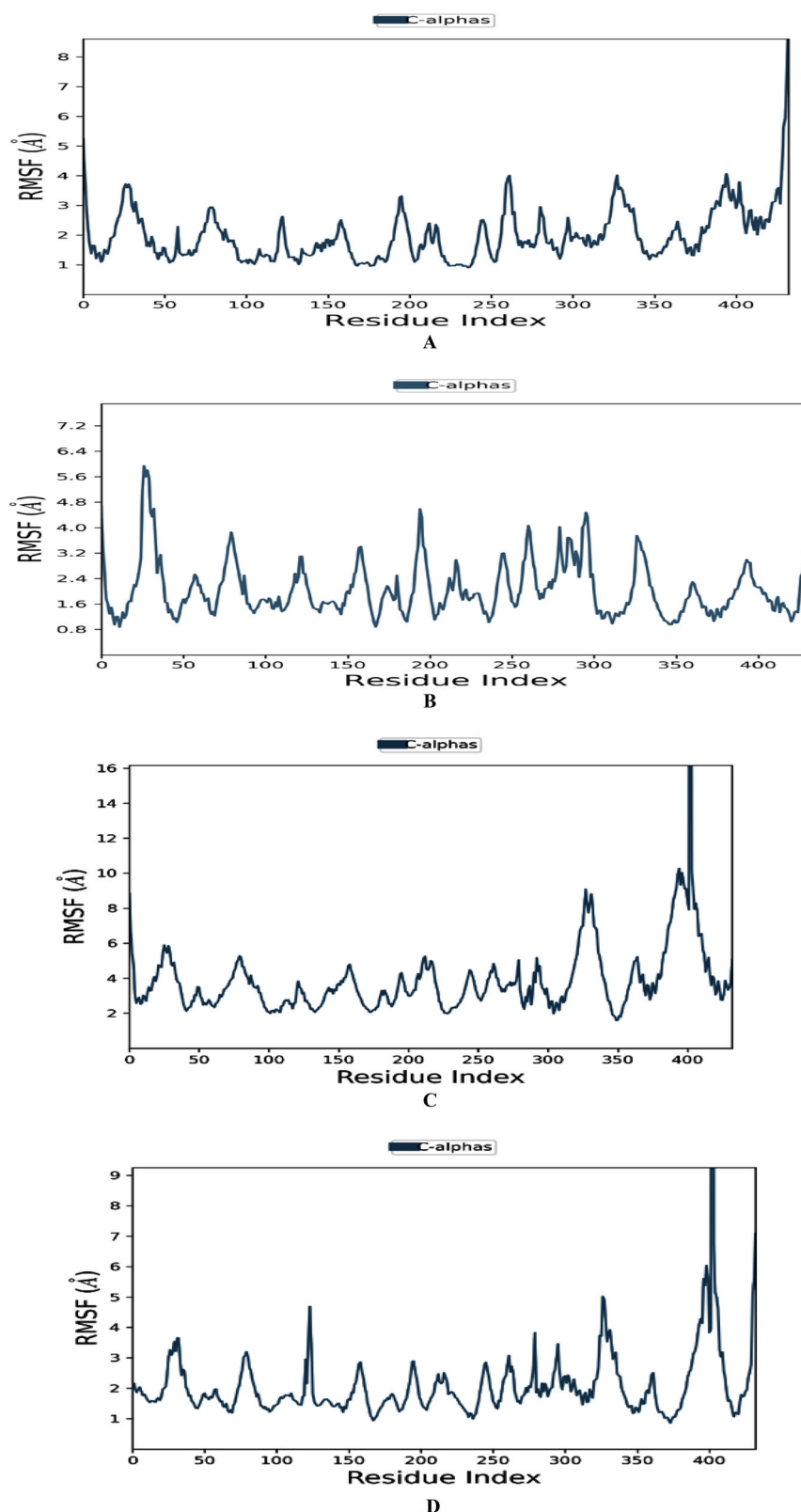


Figure 3. (A) RMSF plot of *heterodimeric non-simulated* ETX (wild)-MAL complex in MD simulation study. (B) RMSF plot of heterodimeric *non-simulated* ETX (mutated)-MAL complex in MD simulation study. (C) RMSF plot of heterodimeric *pre-simulated* ETX (wild)-MAL complex in MD simulation study. (D) RMSF plot of heterodimeric *pre-simulated* ETX (mutated)-MAL complex in MD simulation study.

of pre-simulated ETX-(wild and mutated)-MAL complex states but with the change in the interacting residue. This may be due to change in the position of PPI interactions during MDS which reflects attaining and losing of potential interactions against the targeted protein during the course of simulation time.

Principal component analysis (PCA)

The covariance matrix of the backbone atoms in every simulation protocol was used to set and constrain the flexibility of the Apo and Holo states. The motion of the Apo and Holo

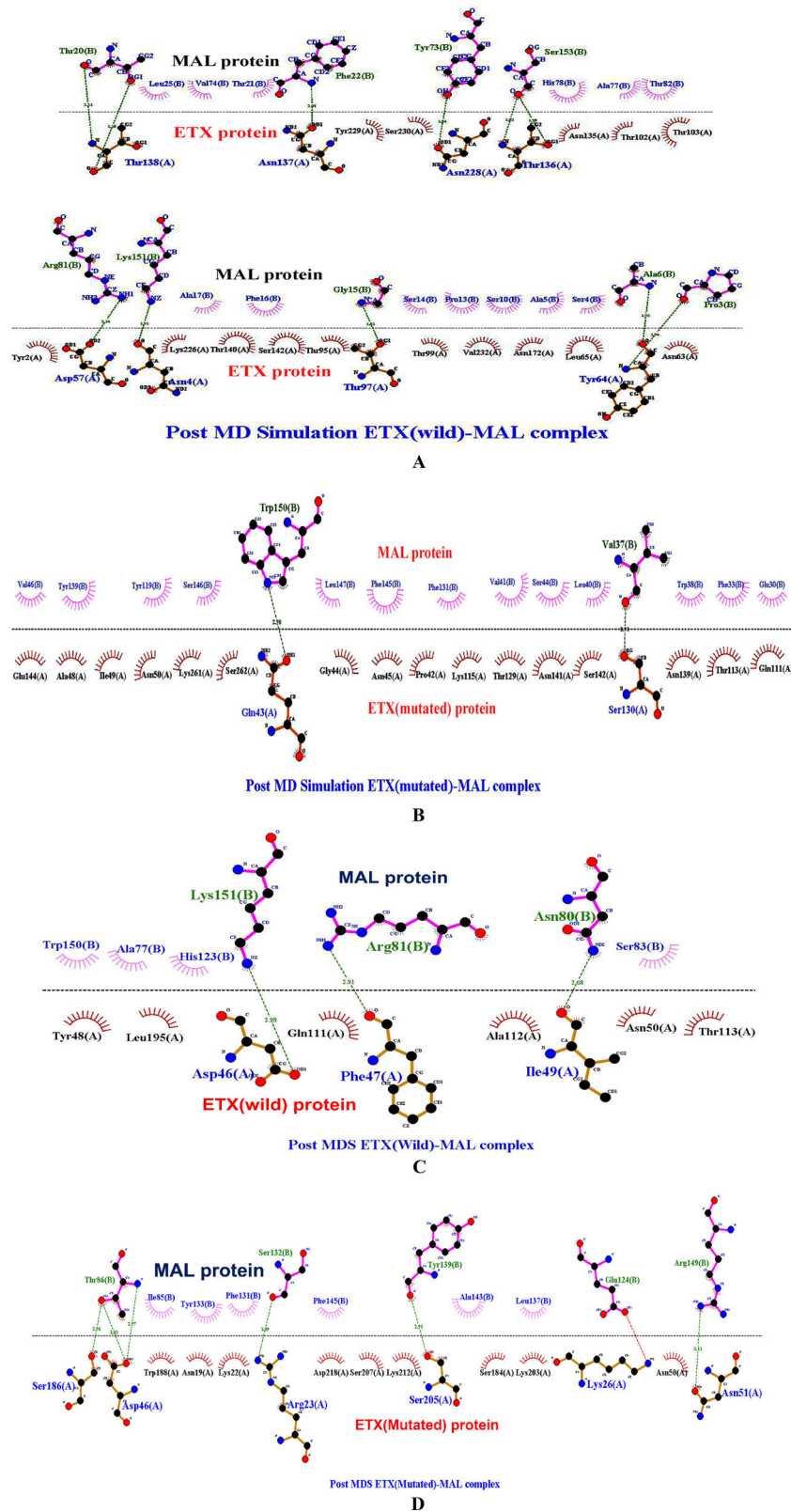


Figure 4. (A) The heterodimeric non-simulated ETX (wild)-MAL complex formed intermolecular hydrogen bonds, electrostatic interactions, and hydrophobic contacts after the MD simulations. The image is drawn by DIMPLOT tool. (B) The heterodimeric non-simulated ETX (mutated)-MAL complex formed intermolecular hydrogen bonds, electrostatic interactions, and hydrophobic contacts after the MD simulations. The image is drawn by DIMPLOT tool. (C) The heterodimeric pre-simulated ETX (wild)-MAL complex formed intermolecular hydrogen bonds, electrostatic interactions, and hydrophobic contacts after the MD simulations. The image is drawn by DIMPLOT tool. (D) The heterodimeric pre-simulated ETX (mutated)-MAL complex formed intermolecular hydrogen bonds, electrostatic interactions, and hydrophobic contacts after the MD simulations. The image is drawn by DIMPLOT tool.

states in phase space was captured by the trajectory projections from PC1 and PC2. The projection of trajectories onto the first two principal components (PC1 and PC2) showed

the motion of Apo and Holo state of the wild and mutated heterodimeric PPI complex in phase space, as depicted in Figure 5(A)–(G).

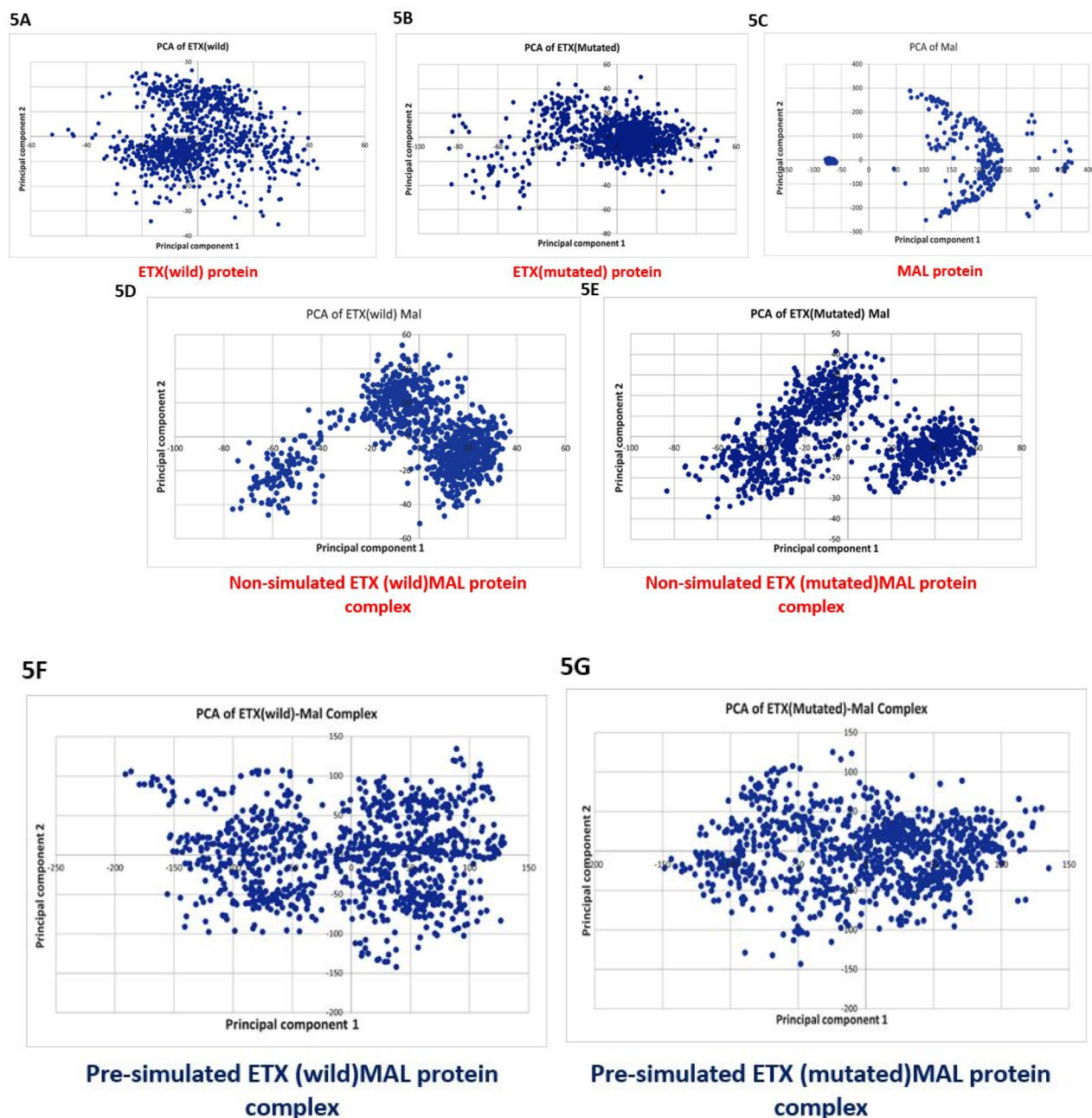


Figure 5. The cloud represents the projection of trajectories (PC1 and PC2). PCA of (A) ETX (wild), (B)ETX (mutated), (C) MAL, (D) Heterodimeric non-simulated ETX (wild)-MAL complex, (E) Heterodimeric non-simulated ETX (mutated)-MAL complex, (F) Heterodimeric pre-simulated ETX (wild) MAL complex and (G) Heterodimeric pre-simulated ETX (mutated) MAL complex.

The scattering cloud of PCA plots represents higher flexibility in ETX (mutated) compared to ETX (wild), heterodimeric non-simulated ETX (mutated)-MAL complex compared to heterodimeric non-simulated ETX (wild)-MAL complex, but in case of heterodimeric pre-simulated ETX (wild)-MAL complex and heterodimeric pre-simulated ETX (mutated)-MAL complex there was a small flexibility, this may be due to motion and remotion of arrangements of atoms during the dual time course of 100 ns simulation time frame. The 'Cross-correlation matrix' of the $C\alpha$ -displacement showed that all residues in the 'ETX (wild and mutated)' protein 'heterodimeric ETX-Mal complex (non- and pre-simulated)' suffer both negatively (shown in blue colors) and positively (shown in red shades) associated motions (Figure 6A–G), which supports the protein's random movement.

The vectorial representation of the individual components indicated the direction of motion. The projection vectors displayed the majority of internal and external motions. After graphing, sharp porcupine plots curves (Figure 7A–G). The porcupine projection depicted inward motion/projection non-simulated ETX (wild)-MAL complex, and outward projection in heterodimeric pre-simulated ETX (mutated)-MAL complex, which represent the change in the motion and flexibility. Like wise outward motion/projection in heterodimeric pre-simulated ETX (wild)-MAL complex, and inward projection in heterodimeric pre-simulated ETX (mutated)-MAL complex, this may be due to motion and remotion of arrangements of atoms during the dual time course of 100 ns simulation time frame.

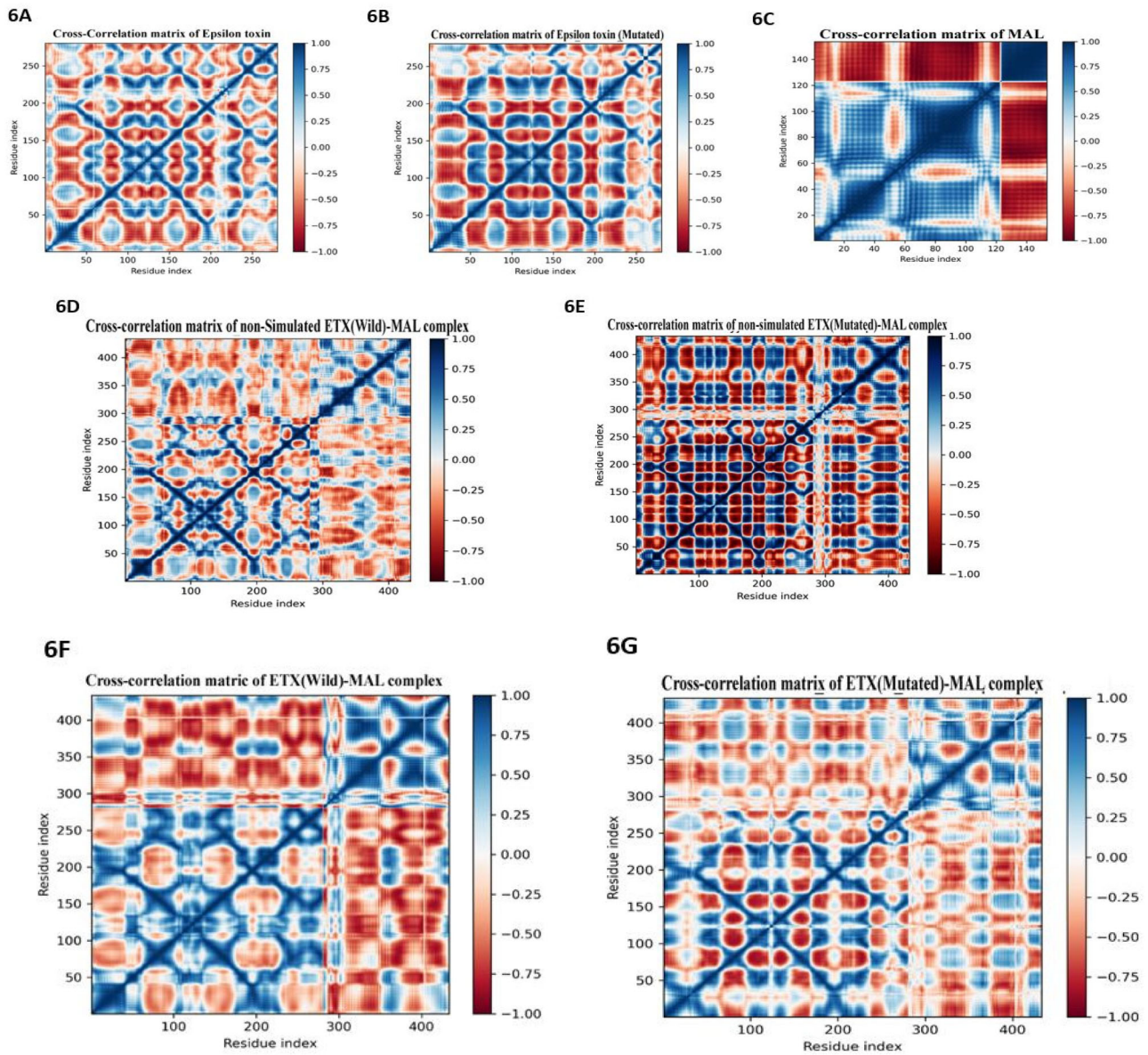


Figure 6. Comparative study of cross-correlation matrices of backbone atoms of (A) ETX (wild), (B) ETX (mutated), (C) MAL, (D) Heterodimeric non-simulated ETX (wild)-MAL complex, (E) Heterodimeric non-simulated ETX (mutated)-MAL complex, (F) Heterodimeric pre-simulated ETX (wild) MAL complex and (G) Heterodimeric pre-simulated ETX (mutated) MAL complex.

Discussion

Pathogenesis of enterotoxaemia is due to the toxins produced by *C. perfringens* and the type of toxins produced are according to its toxinotypes viz., A, B, C, D and E and later two more toxinotypes F and G were included (Pawaiya et al., 2020). The key toxin being a pore forming toxin viz., epsilon toxin (ETX) is produced by *C. perfringens* type B and D. The disease is predisposed by change in the gut environment to anaerobic medium by carbohydrate-rich grain diet or predisposing factors like tapeworm infestations (Singh et al., 2018). The anaerobic gut environment aids in the multiplication of *C. perfringens* and elaboration of its toxins especially the most virulent ETX (Gangwar et al., 2022). The epsilon toxin is initially released as a protoxin but gets activated upon proteolytic cleavage by proteases like trypsin or chymotrypsin which eventually binds to the host cell receptors. Many

researchers in the past studied the pathological effects of epsilon toxin which includes enterocolitis, vascular endothelial damage leading to edema in lungs, brain, kidneys etc. (Kumar et al., 2019; Uzal & Kelly, 1998). These studies aided in understanding of the histopathology and cellular events induced by ETX eventually leading to the ET in domestic animals. Also various molecular events in terms of transcriptional response in hosts at gene level were studied, but the receptor level interaction of epsilon toxin still requires more light. Also, the cellular events after the binding of the ligand to the host receptor which includes oligomerization and pore formation have been well studied recently, besides ETX deletion mutants (Etx- Δ S188-F196 and Etx- Δ V108-F135) with mutation in the binding and insertion domains which affected the pore-forming ability were generated in a wet-lab study previously (Dorca-Arévalo et al., 2022). Although the ETX-host receptor interaction and

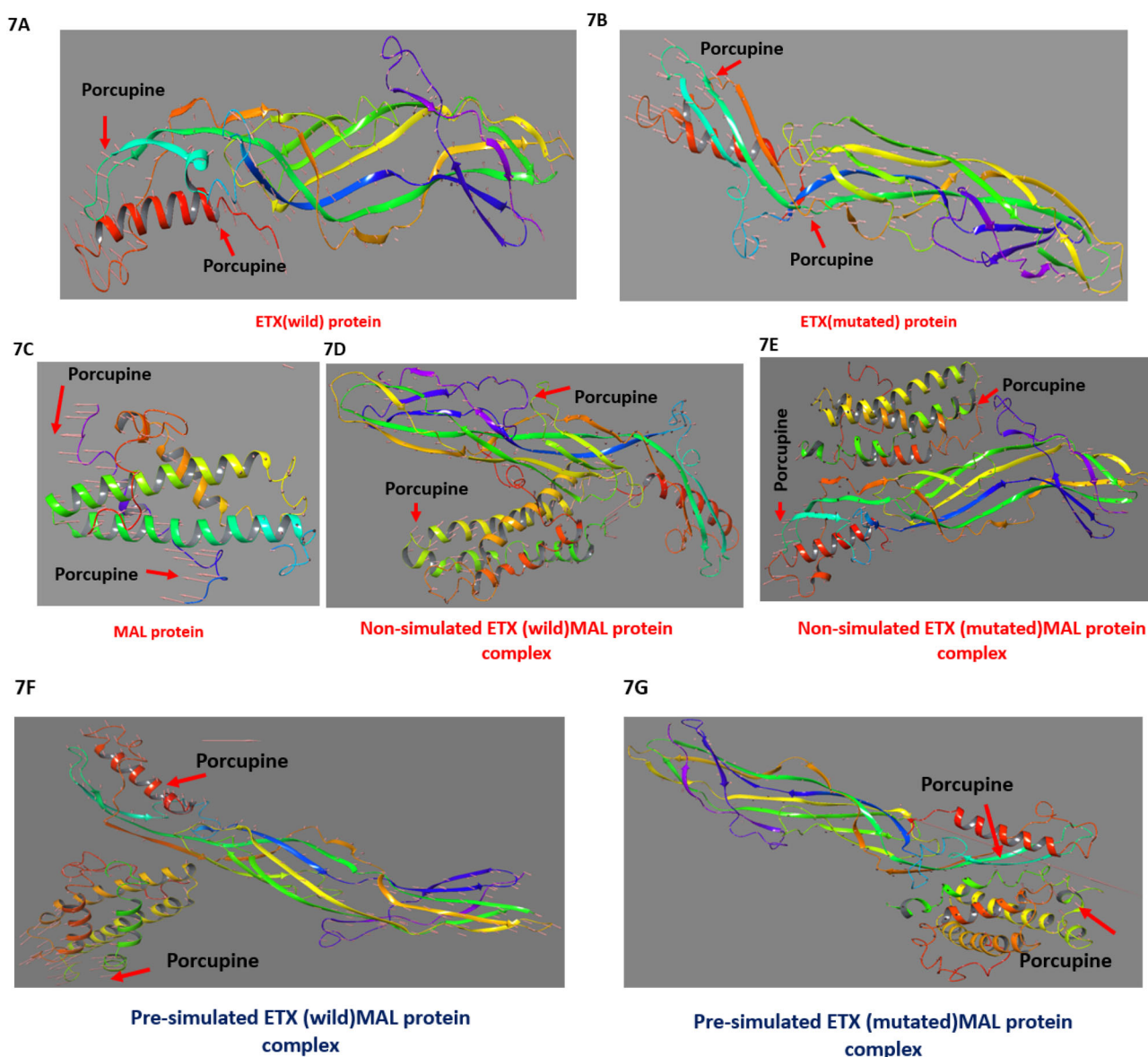


Figure 7. Comparative study of porcupine plot of vectorial motion of (A) ETX (wild), (B) ETX (mutated), (C) MAL, (D) Heterodimeric non-simulated ETX (wild)-MAL complex, (E) Heterodimeric non-simulated ETX (mutated)-MAL complex, (F) Heterodimeric pre-simulated ETX (wild) MAL complex and (G) Heterodimeric pre-simulated ETX (mutated) MAL complex.

the molecular events were elucidated in the past (Manni et al., 2015), but the actual mechanism underlying the binding process was not completely understood. Khalili et al. (2017) conducted an *in silico* study in the past to assess the ETX and its receptors HAVCR1 and MAL and found the involvement of aromatic amino acid residues in the Hydrogen bond with effective binding. But modulation in the binding activity of receptor protein due to tweaking of the ligand region has not been studied *in silico* and not explored yet. Hence, in the current computational assisted study we have conducted the molecular dynamics based analysis of the receptor 'MAL' protein and its interaction with 'wild' as well as 'mutant' epsilon toxin. The ligand ETX is known to contain aromatic amino acid residues which aids in the primary interaction with the host receptors, and in the current study the aromatic residues (tyrosine/phenylalanine) were mutated to aliphatic residues (alanine) in order to study its effect on the host receptors.

The ETX has three domains I, II and III, of which domain I contains aromatic acids like tryptophan and multiple tyrosine residues which contribute to the receptor binding (Dorca-Arévalo et al., 2022). MD simulations have been conducted in the current study for ETX (wild)-MAL and ETX (mutated)-MAL complexes. The PPI heterodimeric ETX (mutated)-MAL protein complex simulation portrayed a lesser number of H bonds with decreased interaction with the host protein. A similar picture was observed in a wet-lab based previous study involving a deletion mutant of epsilon toxin (Etx-DS188-F196) that lacks the loop forming domain 1 which portrayed major differences in the binding pattern in comparison with the wild-type ETX (Dorca-Arévalo et al., 2022).

Another host cell receptor Hepatitis A virus cellular receptor I (HAVCR1) and its interaction was studied previously in a wet-lab study which reported four induced mutations at tyrosine residues 29,30, 36 and 196 which were substitute

with Glutamic acid affecting the host cell permeability and cytotoxicity). This reiterates the fact that substitution of certain aromatic amino acid residues with aliphatic residues could lead to weakened the binding to host receptor as per our findings with the ETX–MAL receptor PPI. Similarly another study in the past (Bokori-Brown et al., 2013) that altered the surface amino acid residues of ETX viz., Tyrosine residues 16, 20, 29, 30, 36 and 196 were all mutated to Alanine (ETX-H149A) in the domain-I which considerably reduced its binding and cytotoxicity to MDCK.2 cells.

Conclusion

The cellular events that leads to the development of Enterotoxaemia is very important to understand the pathogenesis, but the structural and functional analysis governing the Epsilon toxin and host cell interaction is a key for the initiation and development of the disease. The cytotoxic effect caused by ETX again depends upon the binding to the cell and their protein-protein interaction. Hence, we tried to find an answer to this key question, as to how the alteration in the functional residues of epsilon toxin modulated the receptor binding through a computational approach. The epsilon toxin that contains three domains among which the domain-I and II contain essential aromatic residues are key to the cellular binding. In the current study, we altered 10 aromatic amino acid residues in these domains to aliphatic residues and found significant reduction in the binding efficiency and hydrogen bonds compared to the wild type ETX-MAL during protein-protein interactions. A snapshot into the molecular events during interaction of ETX-MAL complex has thrown light on the functional facets of the cellular pathogenesis. The findings from this study could definitely provide a much needed impetus in designing the novel vaccine for Enterotoxaemia in goats.

Disclosure statement

The authors have no conflicts of interest to declare.

Funding

This work was supported by Indian Council of Agricultural Research, Ministry of Agriculture and 743 Farmers' Welfare Govt. of India, CABIN grant (F. no. Agril. Edn.4-1/2013-A&P). The funding organization has not played any role in the study design or the preparation of the manuscript.

Data availability statement

The data supporting the conclusion of this study are available from the corresponding author.

Authors' contributions

SK and KG contributed to conception and design of the research. SKB, SK and SM performed the experiments. SK, SKB and KG drafted the manuscript. SK, KG, SKB, ACS, RP, UBA, RSP and AR did review and editing. All authors contributed to manuscript revision, read and approved the submitted version.

References

- Aier, I., Varadwaj, P. K., & Raj, U. (2016). Structural insights into conformational stability of both wild-type and mutant EZH2 receptor. *Scientific Reports*, 6, 34984. <https://doi.org/10.1038/srep34984>
- Blanch, M., Dorca-Arévalo, J., Not, A., Cases, M., Gomez de Aranda, I., Martínez-Yélamos, A., Martínez-Yélamos, S., Solsona, C., & Blasi, J. (2018). The cytotoxicity of epsilon toxin from *Clostridium perfringens* on lymphocytes is mediated by MAL protein expression. *Molecular and Cellular Biology*, 38(19), e00086-18. <https://doi.org/10.1128/MCB.00086-18>
- Bokori-Brown, M., Kokkinidou, M. C., Savva, C. G., Fernandes da Costa, S., Naylor, C. E., Cole, A. R., Moss, D. S., Basak, A. K., & Titball, R. W. (2013). *Clostridium perfringens* epsilon toxin H149A mutant as a platform for receptor binding studies. *Protein Science*, 22(5), 650–659. <https://doi.org/10.1002/pro.2250>
- Colovos, C., & Yeates, T. O. (1993). Verification of protein structures: Patterns of nonbonded atomic interactions. *Protein Science*, 2(9), 1511–1519. <https://doi.org/10.1002/pro.5560020916>
- Dorca-Arévalo, J., Gómez de Aranda, I., & Blasi, J. (2022). New mutants of epsilon toxin from *Clostridium perfringens* with an altered receptor-binding site and cell-type specificity. *Toxins*, 14(4), 288. <https://doi.org/10.3390/toxins14040288>
- Durrant, J. D., & McCammon, J. A. (2011). Molecular dynamics simulations and drug discovery. *BMC Biology*, 9(1), 1–9. <https://doi.org/10.1186/1741-7007-9-71>
- Fennessey, C. M., Sheng, J., Rubin, D. H., & McClain, M. S. (2012). Oligomerization of *Clostridium perfringens* epsilon toxin is dependent upon caveolins 1 and 2. *PLoS One*, 7(10), e46866. <https://doi.org/10.1371/journal.pone.0046866>
- Finnie, J. W., & Uzal, F. A. (2022). Pathology and pathogenesis of brain lesions produced by *clostridium perfringens* type D epsilon toxin. *International Journal of Molecular Sciences*, 23(16), 9050. <https://doi.org/10.3390/ijms23169050>
- Gangwar, N. K., Pawaiya, R. V. S., Gururaj, K., Andani, D., Kumar, A., Singh, R., & Singh, A. P. (2022). Enterocolitis in goats associated with enterotoxaemia in the perspective of two toxins: Epsilon toxin and beta-2 toxin – An immunohistochemical and molecular study. *Comparative Immunology, Microbiology and Infectious Diseases*, 87, 101837. <https://doi.org/10.1016/j.cimid.2022.101837>
- Hooft, R. W. W., Vriend, G., Sander, C., & Abola, E. E. (1996). Errors in protein structures. *Nature*, 381(6580), 272–272. <https://doi.org/10.1038/381272a0>
- Khalili, S., Jahangiri, A., Hashemi, Z. S., Khalesi, B., Mard-Soltani, M., & Amani, J. (2017). Structural pierce into molecular mechanism underlying *Clostridium perfringens* Epsilon toxin function. *Toxicon*, 127, 90–99. <https://doi.org/10.1016/j.toxicon.2017.01.010>
- Kumar, R., Gururaj, K., Pawaiya, R. V. S., Mishra, A. K., Chaturvedi, V., Varshney, M., Andani, D., Jena, D., Sharma, A., Gangwar, N. K., & Singh, R. (2019). Pathology of experimental *Clostridium perfringens* type D enterotoxaemia in goats.
- Laskowski, R. A., MacArthur, M. W., Moss, D. S., & Thornton, J. M. (1993). PROCHECK: A program to check the stereochemical quality of protein structures. *Journal of Applied Crystallography*, 26(2), 283–291. <https://doi.org/10.1107/S0021889892009944>
- Manni, M. M., Sot, J., & Goñi, F. M. (2015). Interaction of *Clostridium perfringens* epsilon-toxin with biological and model membranes: A putative protein receptor in cells. *Biochimica et Biophysica Acta*, 1848(3), 797–804. <https://doi.org/10.1016/j.bbame.2014.11.028>
- Mathur, D. D., Deshmukh, S., Kaushik, H., & Garg, L. C. (2010). Functional and structural characterization of soluble recombinant epsilon toxin of *Clostridium perfringens* D, causative agent of enterotoxaemia. *Applied Microbiology and Biotechnology*, 88(4), 877–884. <https://doi.org/10.1007/s00253-010-2785-y>
- Mitchell, A., Chang, H.-Y., Daugherty, L., Fraser, M., Hunter, S., Lopez, R., McAnulla, C., McMenamin, C., Nuka, G., Pesseat, S., Sangrador-Vegas, A., Scheremetjew, M., Rato, C., Yong, S.-Y., Bateman, A., Punta, M., Attwood, T. K., Sigrist, C. J. A., Redaschi, N., ... Finn, R. D. (2015). The InterPro protein families database: The classification resource after 15 years. *Nucleic Acids Research*, 43(Database issue), D213–21. <https://doi.org/10.1093/nar/gku1243>
- Nagahama, M., Seike, S., Ochi, S., Kobayashi, K., & Takehara, M. (2020). *Clostridium perfringens* epsilon-toxin impairs the barrier function in

- MDCK cell monolayers in a Ca^{2+} -dependent manner. *Toxins*, 12(5), 286. <https://doi.org/10.3390/toxins12050286>
- Pawaiya, R. S., Gururaj, K., Gangwar, N. K., Singh, D. D., Kumar, R., & Kumar, A. (2020). The challenges of diagnosis and control of enterotoxaemia caused by *Clostridium perfringens* in small ruminants. *Advances in Microbiology*, 10(05), 238–273. <https://doi.org/10.4236/aim.2020.105019>
- Pontius, J., Richelle, J., & Wodak, S. J. (1996). Deviations from standard atomic volumes as a quality measure for protein crystal structures. *Journal of Molecular Biology*, 264(1), 121–136. <https://doi.org/10.1006/jmbi.1996.0628>
- Singh, D. D., Pawaiya, R. V. S., Gururaj, K., Gangwar, N. K., Mishra, A. K., Singh, R., Andani, D., & Kumar, A. (2018). Detection of *Clostridium perfringens* toxinotypes, enteropathogenic *E. coli*, Rota and corona viruses in the intestine of neonatal goat kids by molecular techniques. *The Indian Journal of Animal Sciences*, 88(6), 655–661. <https://doi.org/10.56093/ijans.v88i6.80863>
- Uzal, F. A., & Kelly, W. R. (1998). Experimental *Clostridium perfringens* type D enterotoxemia in goats. *Veterinary Pathology*, 35(2), 132–140. <https://doi.org/10.1177/030098589803500207>
- Vaguine, A. A., Richelle, J., & Wodak, S. J. (1999). SFCHECK: A unified set of procedure for evaluating the quality of macromolecular structure-factor data and their agreement with atomic model. *Acta Crystallographica, Section D, Biological Crystallography*, 55(Pt 1), 191–205. <https://doi.org/10.1107/S0907444998006684>
- Weng, X., Hamel, L., Martin, L. M., & Peckham, J. (2005). A genetic algorithm for energy minimization in bio-molecular systems. *Evolutionary Computation*, The 2005 IEEE Congress (Vol. 1, pp. 49–56).
- Xu, D., & Zhang, Y. (2011). Improving the physical realism and structural accuracy of protein models by a two-step atomic-level energy minimization. *Biophysical Journal*, 101(10), 2525–2534. <https://doi.org/10.1016/j.bpj.2011.10.024>
- Zhang, Y. (2008). I-TASSER server for protein 3D structure prediction. *BMC Bioinformatics*, 9, 40. <https://doi.org/10.1186/1471-2105-9-40>
- Zhang, J., Liang, Y., & Zhang, Y. (2011). Atomic-level protein structure refinement using fragment-guided molecular dynamics conformation sampling. *Structure (London, England: 1993)*, 19(12), 1784–1795. <https://doi.org/10.1016/j.str.2011.09.022>